

# Development of a NanoBRET Assay Platform to Detect Intracellular Ligands for the Chemokine Receptors CCR6 and CXCR1

Max E. Huber<sup>+</sup>,<sup>[a]</sup> Silas L. Wurnig<sup>+</sup>,<sup>[b]</sup> Aurélien F. A. Moumbock,<sup>[c]</sup> Lara Toy,<sup>[a]</sup> Evi Kostenis,<sup>[d]</sup> Ana Alonso Bartolomé,<sup>[e, f]</sup> Martyna Szpakowska,<sup>[e]</sup> Andy Chevigné,<sup>[e]</sup> Stefan Günther,<sup>[c]</sup> Finn K. Hansen,<sup>\*,[b]</sup> and Matthias Schiedel<sup>\*,[a, g]</sup>

A conserved intracellular allosteric binding site (IABS) was recently identified at several G protein-coupled receptors (GPCRs). This target site allows the binding of allosteric modulators and enables a new mode of GPCR inhibition. Herein, we report the development of a NanoBRET-based assay platform based on the fluorescent ligand LT221 (5), to detect intracellular binding to CCR6 and CXCR1, two chemokine receptors that have been pursued as promising drug targets in inflammation and immuno-oncology. Our assay platform enables cell-free as well as cellular NanoBRET-based binding studies in a nonisotopic and straightforward manner. By combining this screening platform with a previously reported

CXCR2 assay, we investigated CXCR1/CXCR2/CCR6 selectivity profiles for both known and novel squaramide analogues derived from navarixin, a known intracellular CXCR1/CXCR2 antagonist and phase II clinical candidate for the treatment of pulmonary diseases. By means of these studies we identified compound 10, a previously reported *tert*-butyl analogue of navarixin, as a low nanomolar intracellular CCR6 antagonist. Further, our assay platform clearly indicated intracellular binding of the CCR6 antagonist PF-07054894, currently evaluated in phase I clinical trials for the treatment of ulcerative colitis, thereby providing profound evidence for the existence and the pharmacological relevance of a druggable IABS at CCR6.

## Introduction

G protein-coupled receptors (GPCRs) are the largest family of membrane receptors, mediate signaling across the cell membrane, and regulate a plethora of physiological and pathophysiological processes. As a consequence of their involvement in the development and progression of various diseases, GPCRs are pharmaceutically highly relevant and represent the primary drug targets for approximately one third of all available medication.<sup>[1]</sup> The vast majority of known GPCR ligands bind to

an orthosteric site of the heptahelical transmembrane receptor that is located within the helical bundle and accessible from the extracellular environment. In addition to this orthosteric site, several allosteric ligand binding sites at GPCRs were recently described.<sup>[2]</sup> One of these sites is the conserved intracellular allosteric binding site (IABS) that enables the binding of small-molecule negative modulators and has recently been identified by X-ray co-crystallography at the chemokine receptors CCR2,<sup>[3]</sup> CCR7,<sup>[4]</sup> CCR9,<sup>[5]</sup> CXCR2,<sup>[6]</sup> as well as at the beta-2 adrenergic receptor ( $\beta_2$ AR).<sup>[7]</sup> Additionally, growing evidence supports the

[a] M. E. Huber,<sup>+</sup> L. Toy, Prof. Dr. M. Schiedel  
Department of Chemistry and Pharmacy, Medicinal Chemistry  
Friedrich-Alexander-University Erlangen-Nürnberg  
Nikolaus-Fiebiger-Straße 10, 91058 Erlangen, Germany  
E-mail: matthias.schiedel@tu-braunschweig.de  
matthias.schiedel@fau.de

[b] S. L. Wurnig,<sup>+</sup> Prof. Dr. F. K. Hansen  
Department of Pharmaceutical & Cell Biological Chemistry, Pharmaceutical  
Institute  
University of Bonn  
An der Immenburg 4, 53121 Bonn, Germany  
E-mail: finn.hansen@uni-bonn.de

[c] Dr. A. F. A. Moumbock, Prof. Dr. S. Günther  
Institute of Pharmaceutical Sciences  
Albert-Ludwigs-Universität Freiburg  
Hermann-Herder-Straße 9, 79104 Freiburg, Germany

[d] Prof. Dr. E. Kostenis  
Molecular, Cellular and Pharmacobiology Section, Institute for Pharmaceuti-  
cal Biology  
University of Bonn  
Nussallee 6, 53115 Bonn, Germany

[e] A. Alonso Bartolomé, Dr. M. Szpakowska, Dr. A. Chevigné  
Immuno-Pharmacology and Interactomics, Department of Infection and  
Immunity  
Luxembourg Institute of Health  
rue Henri Koch 29, 4354 Esch-sur-Alzette, Luxembourg

[f] A. Alonso Bartolomé  
Faculty of Science, Technology and Medicine  
University of Luxembourg  
2 Avenue de l'Université, L-4365 Esch-sur-Alzette, Luxembourg

[g] Prof. Dr. M. Schiedel  
Institute of Medicinal and Pharmaceutical Chemistry  
Technische Universität Braunschweig  
Beethovenstraße 55, 38106 Braunschweig, Germany

[\*] M. E. H. and S. L. W. contributed equally to this work.

Supporting information for this article is available on the WWW under  
<https://doi.org/10.1002/cmdc.202400284>

© 2024 The Authors. ChemMedChem published by Wiley-VCH GmbH. This is  
an open access article under the terms of the Creative Commons Attribution  
Non-Commercial NoDerivs License, which permits use and distribution in  
any medium, provided the original work is properly cited, the use is non-  
commercial and no modifications or adaptations are made.

existence of a druggable IABS at several other GPCRs, including CCR1 and CXCR1.<sup>[8]</sup> Ligands that target the IABS feature a new dual mode of specific GPCR inhibition, which is characterized by a stabilization of the inactive receptor conformation and a steric blockade of intracellular transducer (i.e., G protein and/or  $\beta$ -arrestin) binding.<sup>[3–7]</sup> Owing to their unique mechanism, ligands targeting the IABS open new avenues to modulate receptor function and to generate selectivity. Making use of this new approach of specific GPCR inhibition is particularly attractive for GPCR families such as the chemokine receptors, where the development of orthosteric ligands has shown very limited therapeutic success.<sup>[9]</sup> Several intracellular chemokine receptor antagonists, including the CXCR1/CXCR2-targeted navarixin (1), have progressed to clinical trials,<sup>[10]</sup> thus highlighting the immense potential of intracellular GPCR inhibition.

However, neither the discovery nor the optimization of intracellular allosteric GPCR inhibitors is straightforward. Their complex pharmacology and probe dependence often requires labor-intensive testing in various functional assays, which complicates standard high-throughput screening (HTS) approaches.<sup>[11]</sup> So far, radioligand ligand binding assays were primarily utilized to demonstrate target engagement for intracellular GPCR modulators.<sup>[5,12]</sup> Although radioligand binding assays are powerful methods, in particular with respect to their high sensitivity, several drawbacks are associated with this technology. General drawbacks of isotopic methods are special safety precautions, the requirement for specialized laboratories, permits for radioisotope handling, the high cost for the procurement of radiolabeled tracers, expensive disposal of radioactive waste, and the need for often laborious (heterogeneous) assay protocols, including washing steps to remove the unbound radioligand prior to assay readout.<sup>[13]</sup> The latter is also the reason why radioligand binding assays are often not well-suited for kinetic measurements with a continuous readout, the detection of low-affinity binders, or cellular target engagement studies for intracellular binding sites, such as the IABS at GPCRs. To leverage drug discovery campaigns in the area of intracellular GPCR ligands, we and others have recently developed small-molecule fluorescent tracers targeting the IABS of several GPCRs, including CCR2,<sup>[14]</sup> CCR9,<sup>[15]</sup> and CXCR2.<sup>[8b,13a,16]</sup> These fluorescent ligands enabled cell-free as well as cellular NanoBRET-based binding studies in a nonisotopic and high-throughput manner. The beauty of proximity based technologies like NanoBRET is that they not only provide information on the event but also on the location of ligand binding, since a resonance energy transfer is only possible over very short distances (< 10 nm).<sup>[17]</sup> Thus, a NanoBRET setup with a GPCR that is labelled at its intracellular C-terminus with a NanoLuc Luciferase (Nluc) allows both the detection of intracellular binders and provides evidence for the existence of an intracellular allosteric binding site at the studied receptor. The latter aspect is especially interesting for GPCRs, for which a druggable IABS has been suggested but not yet finally corroborated by means of X-ray and cryo-EM co-structures, respectively, or mutational studies.

For the chemokine receptors CXCR1 and CCR6, two promising drug targets in inflammation and immuno-

oncology,<sup>[10a,18]</sup> the discovery of high affinity squaramide-based antagonists (e.g., navarixin (1) or PF-07054894 (2, Figure 1A))<sup>[18b,d,19]</sup> suggests the existence of an IABS at these receptors, since X-ray co-crystallography studies with the closely related CXCR2 showed that the squaramide substructure substantially contributes to intracellular GPCR binding.<sup>[6]</sup> In the case of CXCR1, our recently reported intracellular CXCR2-targeted fluorescent tracers (3–5, Figure 1B) showed off-target binding to CXCR1,<sup>[8b]</sup> thereby indicating a druggable IABS at CXCR1. Beyond the detection of their off-target affinity for CXCR1, 3–5 were not further applied as molecular tools to study intracellular ligand binding to CXCR1. For CCR6, neither a druggable IABS nor systematic approaches for the discovery of intracellular inhibitors have been reported thus far.

Herein, we aimed for developing a NanoBRET-based assay platform to detect intracellular binding to CCR6 and CXCR1 in a high-throughput and nonisotopic manner. This assay platform was envisaged to enable equilibrium as well as kinetic binding studies in a cell-free and live cell environment, provide further evidence for the existence of a druggable IABS at CCR6 and CXCR1, allow mapping of known CCR6 and CXCR1 ligands to distinct binding sites, and enable the discovery of novel intracellular antagonists for CCR6 and CXCR1.

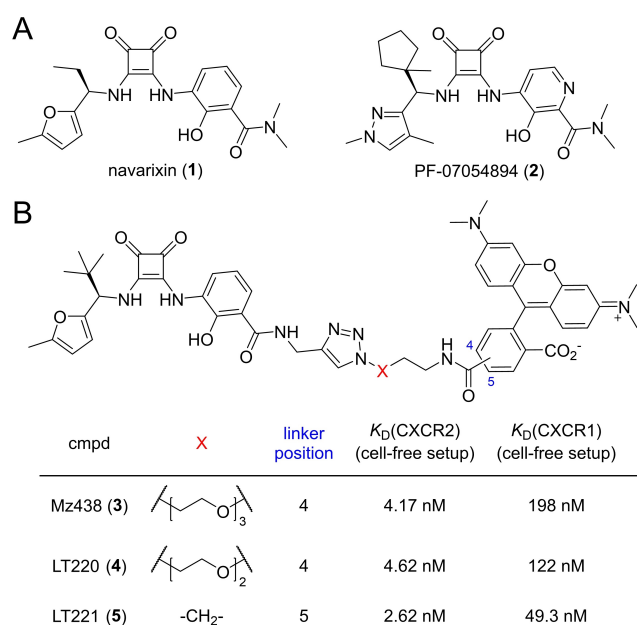


**Figure 1.** A) Chemical structures of the previously reported squaramide-based CXCR1/CXCR2 antagonist navarixin (1) and the CCR6-targeted PF-07054894 (2).<sup>[18b,d]</sup> B) Chemical structures and binding affinities of previously reported fluorescent CXCR2 ligands 3–5 that also showed off-target binding to the closely related CXCR1. Given  $K_D$  values were determined with membrane-based saturation binding assays.<sup>[8b]</sup>

## Results and Discussion

## Assay Development for CXCR1

Based on the knowledge that the previously reported intracellular fluorescent CXCR2 ligands 3–5 show off-target binding to CXCR1 (Figure 1B),<sup>[8b]</sup> we aimed for studying their applicability as tracer molecules to monitor the binding of non-fluorescent ligands to the IABS of CXCR1. To this end, we set up a NanoBRET-based competition binding assay with membranes from HEK293T cells transiently expressing a C-terminally Nluc-tagged CXCR1 construct,<sup>[8b]</sup> hereafter referred to as CXCR1\_Nluc (Figure 2A). As a fluorescent tracer molecule we selected LT221 (5), because this compound showed the highest CXCR1 affinity ( $K_D = 49.3$  nM) among our squaramide-based fluorescent ligands 3–5 (Figure 1B).<sup>[8b]</sup> Using this setup, we determined a  $pK_i$  value of  $7.64 \pm 0.06$  [23.6 nM] for the known dual CXCR1/CXCR2 antagonist navarixin (1, Figures 2B and S1A). This result is in good agreement with the reported  $IC_{50}$  value (36 nM) of 1 for CXCR1.<sup>[18b]</sup> For the linker-ligand conjugate XI (6, Figures 2B and S1A),<sup>[8b]</sup> which features the same CXCR1 binding unit as the fluorescent tracer 5, we detected an even higher CXCR1 affinity with a  $pK_i$  value of  $7.78 \pm 0.07$  [17.3 nM] as compared to 1. This indicates that the attachment of a triazole-based linker in combination with an ethyl to *tert*-butyl switch at the stereogenic center of 1 is well tolerated with respect to CXCR1 affinity. For the low- to sub-nanomolar extracellular orthosteric CXCR1

agonist CXCL8,<sup>[20]</sup> also referred to as IL-8, we detected no significant competition with 5 (Figures 2B and S1A), thereby confirming the previously reported noncompetitive allosteric binding mode of intracellular allosteric chemokine receptor antagonists.<sup>[8b,12a,15]</sup>

To provide further evidence that 5 actually binds to the intracellular face of CXCR1, we performed docking studies with a homology model of CXCR1 that is based on the previously reported co-crystal structure of the closely related CXCR2 in complex with the intracellular antagonist 00767013 (7, PDB ID: 6LFL).<sup>[6]</sup> Our docking experiments suggested that 1 as well as the linker-ligand conjugate 6 should be able to bind to the IABS of CXCR1 in a highly similar manner as observed for the squaramide 7 in the co-structure with CXCR2 (Figure 2C).<sup>[6]</sup> Additionally, we experimentally verified that the resonance energy transfer from the Nluc (donor) to the fluorescent tracer (acceptor) cannot happen across the cell membrane. To this end, we used our well established intracellular fluorescent ligand for CCR9<sup>[13a,15]</sup> that is directly derived from the *bona fide* intracellular CCR9 antagonist vercinon.<sup>[5]</sup> As expected, we detected no significant NanoBRET signal when using the intracellular fluorescent CCR9 ligand in combination with an extracellularly Nluc-tagged CCR9 construct (i.e., FLAG\_Nluc\_CCR9), whereas the combination with an intracellularly Nluc-tagged CCR9 construct (i.e., CCR9\_Nluc) results in a clear NanoBRET signal (Figure S2A–C). Most recently, similar results were also reported for an intracellular fluorescent tracer for the

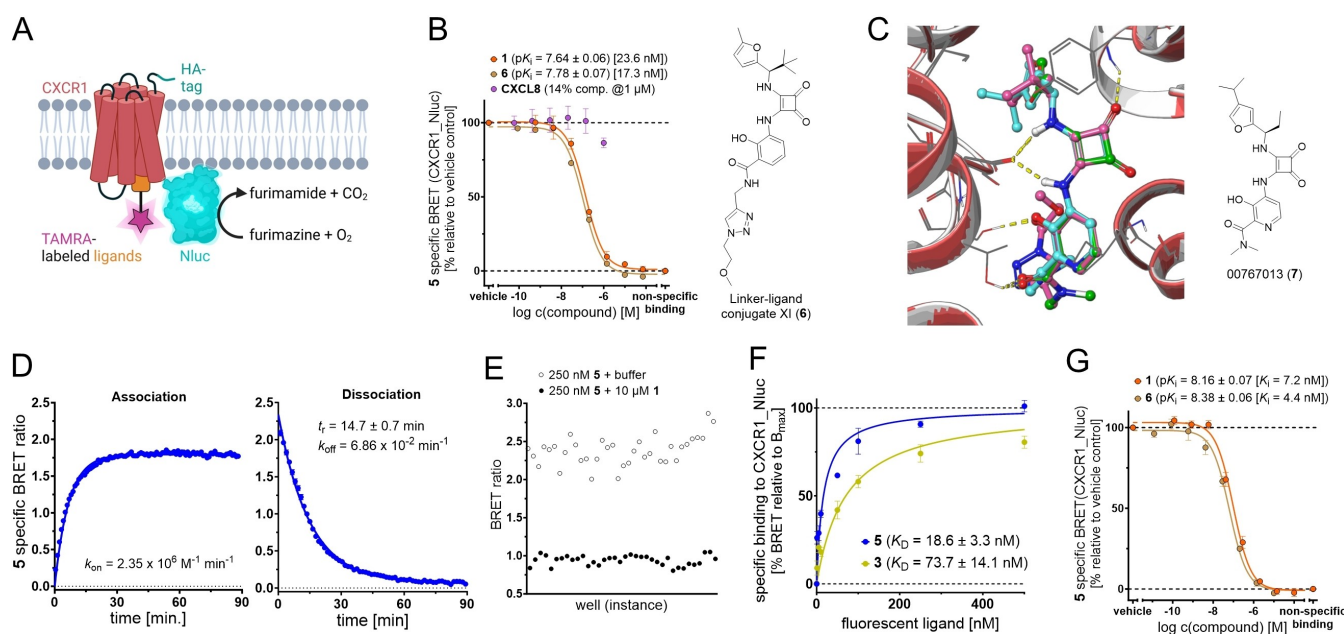


**Figure 2.** Application of LT221 (5) as a fluorescent tool for NanoBRET-based binding studies targeting the IABS of CXCR1. A) Cartoon representation of the NanoBRET strategy to detect binding to the IABS of CXCR1. B) Competition binding curves and determined  $pK_i$  values (mean  $\pm$  SEM, triplicate measurement,  $n \geq 3$ ) for the known CXCR1/CXCR2 antagonist navarixin (1),<sup>[18b]</sup> the linker-ligand conjugate XI (6, chemical structure on the right),<sup>[8b]</sup> and the extracellular orthosteric CXCR1 agonist CXCL8,<sup>[20]</sup> obtained with 5 (250 nM) and CXCR1\_Nluc membranes.  $K_i$  values are given in square brackets. C) Overlay of predicted CXCR1 (red) binding modes for 1 (green) and 6 (purple) with the observed CXCR2 (grey) binding mode of 00767013 (7, cyan, chemical structure on the right, PDB ID: 6LFL).<sup>[6]</sup> D) Kinetic binding studies at room temperature. Representative association and dissociation curves with 5 (50 nM) using CXCR1\_Nluc membranes ( $n = 4$ ). E) Z'-factor determination for the cell-free NanoBRET-based setup using 5 (250 nM) and CXCR1\_Nluc membranes (36-fold determination). F) Saturation binding curve of fluorescent probes 3 and 5 in a cellular NanoBRET-based experiment (mean  $\pm$  SEM, quadruplicate measurement,  $n \geq 4$ ) using HEK293T cells transiently overexpressing CXCR1\_Nluc. G) Cellular competition binding curves and  $pK_i$  values (mean  $\pm$  SEM, quadruplicate measurement) for 1 (orange,  $n = 4$ ) and 6 (beige,  $n = 5$ ) obtained with 5 (250 nM).  $K_i$  values are given in square brackets.

neurotensin receptor type 1 (NTSR1), which was used in combination with intra- and extracellularly Nluc-labelled NTSR1.<sup>[21]</sup> All these data strongly suggest that the resonance energy cannot be transferred across the cell membrane, which further corroborates an intracellular binding of LT221 (**5**) to CXCR1.

To characterize the binding kinetics of **5** to CXCR1, we set up a NanoBRET-based kinetic binding assay (Figure 2D). These measurements resulted in an association rate constant of  $k_{\text{on}} = 2.35 \pm 0.54 \times 10^6 \text{ M}^{-1} \text{ min}^{-1}$ , a dissociation rate constant of  $k_{\text{off}} = 6.86 \pm 0.35 \times 10^{-2} \text{ min}^{-1}$ , a residence time of  $t_r = 14.7 \pm 0.7 \text{ min}$ , and a kinetic  $K_D$  value of  $34.7 \pm 8.1 \text{ nM}$ , which is in good agreement with the reported equilibrium  $K_D$  value of  $49.3 \text{ nM}$ .<sup>[8b]</sup>

In order to assess the quality of our cell-free NanoBRET competition binding assay and its suitability for HTS approaches, we determined a Z'-factor according to Zhang *et al.*<sup>[22]</sup> This resulted in a Z'-factor of 0.75 (Figure 2E), thus indicating that our cell-free NanoBRET assay can be considered as excellent and suitable for HTS approaches.

After having shown that **5** is a valuable tool to study binding to the IABS of CXCR1 in a cell-free setup, we aimed for transferring our NanoBRET binding assay to a live cell environment. Methods to study cellular target engagement are of utmost importance in preclinical drug discovery, since on-target activity of small molecules can be significantly affected when moving from a cell-free to a cellular environment, due to various reasons, including low cell permeability, compound efflux, or off-target binding.<sup>[23]</sup> Because of the intracellular location of the IABS, ligands targeting this site need to pass the plasma membrane to be active in a cellular setup, thus cellular binding assays are highly important for identifying suitable candidates for further development. To the best of our knowledge, no small-molecule tracers have been reported thus far that enabled cellular binding assays for the IABS of CXCR1. For our cellular CXCR1 binding assay we used live HEK293T cells transiently expressing CXCR1\_Nluc. With this cellular setup we determined a  $K_D$  value of  $18.6 \pm 3.3 \text{ nM}$  for **5** (Figures 2F and S1B), thereby demonstrating that **5** is able to pass the cell membrane and bind to CXCR1 at the intracellular side of the receptor. In very good agreement with the previously reported cell-free binding data (Figure 1B), our cell-based CXCR1 assay indicated an approximately 4-fold weaker affinity for the fluorescent tracer **3** ( $K_D = 73.7 \pm 14.1 \text{ nM}$ , Figures 2F and S1C), compared to **5**. Next, we applied **5** in a cell-based competition binding assay to study cellular target engagement for non-fluorescent intracellular CXCR1 ligands. In the course of these studies, we determined a low nanomolar  $K_i$  value for the known dual CXCR1/CXCR2 antagonist **1** ( $pK_i = 8.16 \pm 0.07$  [ $7.2 \text{ nM}$ ]) and a slightly higher affinity for the linker-ligand conjugate **6** ( $pK_i = 8.38 \pm 0.06$  [ $4.4 \text{ nM}$ ], Figures 2G and S1D). This is in line with the affinities determined in the cell-free setup (Figure 2B). Overall, the results from live cell NanoBRET and membrane-based experiments are in very good agreement with each other, thereby indicating that **5** is a suitable tool for studying ligand binding to the IABS of CXCR1 in live cells.

## Assay Development for CCR6

Inspired by reports indicating that ligands featuring a squaramide, a well-known structural motif of intracellular chemokine receptor antagonists,<sup>[6,10b]</sup> are also binding to CCR6,<sup>[18d,19]</sup> we aimed for investigating the suitability of our previously reported squaramide-based ligands **3–5** as fluorescent tracers for CCR6. To monitor binding to the IABS of CCR6 via the NanoBRET technique, we first had to develop suitable CCR6-Nluc fusion proteins (Figure S3A–C). To this end, we genetically attached an Nluc-tag either directly to the intracellular C-terminus of CCR6 or with a GSSG linker between CCR6 and the Nluc-tag (Figures 3A and S3A), in a similar manner as reported for CCR2 or CCR9.<sup>[8b,14–15]</sup> Successful surface expression of CCR6-Nluc fusion proteins, hereafter referred to as CCR6\_Nluc and CCR6\_GSSG\_Nluc, was confirmed by ELISA directed against an N-terminal 3xHAtag (Figure S3B).

In saturation binding experiments using membranes from HEK293T cells transiently expressing CCR6\_Nluc, **5** showed the highest binding affinity among the tested ligands, with a  $K_D$  value of  $38.0 \pm 5.0 \text{ nM}$  (Figures 3B and S3D–F). In combination with the aforementioned observation that a resonance energy transfer cannot happen across the cell membrane (Figure S2), these results strongly suggest both the existence of a druggable IABS at CCR6 and that squaramide-based ligands, such as the fluorescent tracer **5**, are binding to this intracellular binding pocket. Similar to the studies for CXCR1 (see above), we again used docking experiments with a homology model to further support intracellular CCR6 binding of **5**. The predicted binding mode indicates that the CCR6-targeted pharmacophore of **5** binds to the IABS of CCR6 in a very similar manner as reported for the squaramide based ligand 00767013 (**7**) that has been co-crystallized with the closely related CXCR2 (Figure 3C).<sup>[6]</sup> Kinetic binding studies with **5** and CCR6\_Nluc membranes resulted in an association rate constant of  $k_{\text{on}} = 1.38 \pm 0.30 \times 10^6 \text{ M}^{-1} \text{ min}^{-1}$ , a dissociation rate constant of  $k_{\text{off}} = 2.26 \pm 0.22 \times 10^{-2} \text{ min}^{-1}$ , a residence time of  $t_r = 45.5 \pm 4.2 \text{ min}$ , and a kinetic  $K_D$  value of  $18.7 \pm 4.4 \text{ nM}$  (Figure 3D), which is in good agreement with the detected equilibrium  $K_D$  value of  $38.0 \text{ nM}$  (Figure 3B).

Next, we aimed for investigating the suitability of **5** as a tracer to report the binding of nonfluorescent ligands to the IABS of CCR6. In a membrane-based CCR6 competition binding assay both the squaramide-based **1** as well as the linker-ligand conjugate **6** evoked full displacement of **5** from the IABS of CCR6 (Figures 3E and S3G). Interestingly, the linker-ligand conjugate **6** ( $pK_i = 7.99 \pm 0.01$  [ $10.1 \text{ nM}$ ]) showed a much higher CCR6 affinity than **1** ( $pK_i = 5.98 \pm 0.01$  [ $1060 \text{ nM}$ ]), thereby indicating that either the *tert*-butyl or the triazole-based linker moiety of **6** might be responsible for this over 100-fold increase in CCR6 affinity. The sub-nanomolar orthosteric CCR6 agonist CCL20,<sup>[24]</sup> also known as MIP-3 $\alpha$ , evoked no displacement of **5** (Figures 3E and S3G), thereby confirming a noncompetitive allosteric binding mode of **5** to CCR6. This is in agreement with our results obtained for CXCR1 (see above) and the reported literature for other intracellular allosteric chemokine receptor antagonists.<sup>[8b,12a,15]</sup>



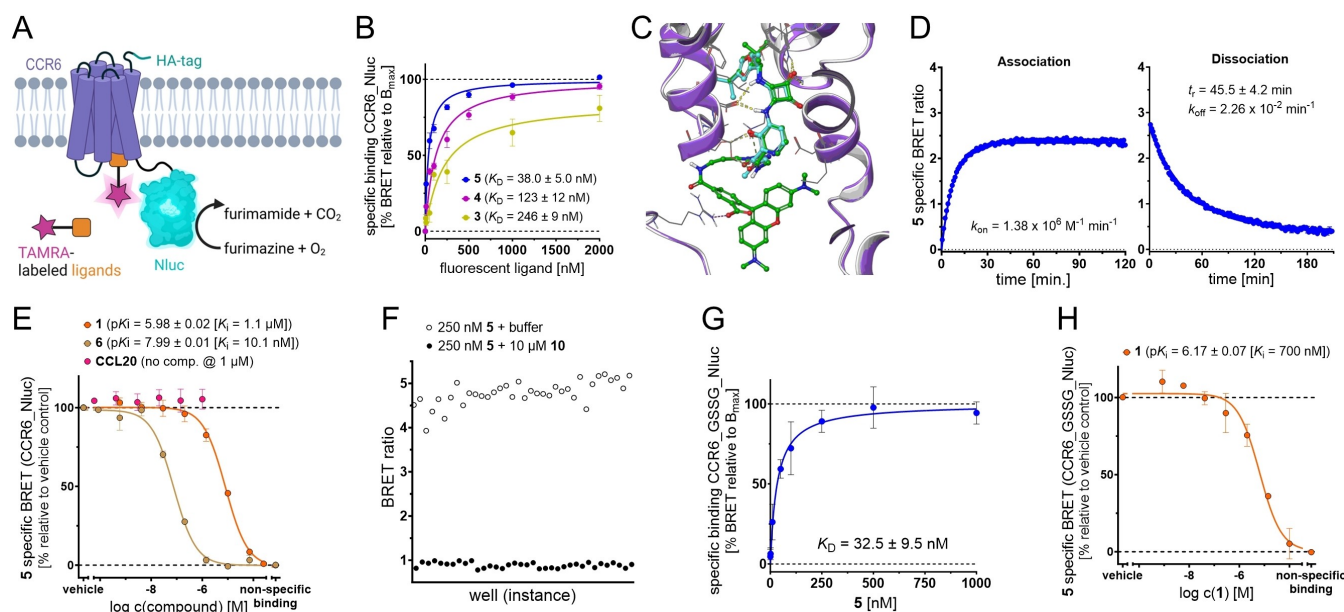


**Figure 3.** Application of LT221 (5) as a fluorescent tool for NanoBRET-based binding studies targeting the IABS of CCR6. A) Cartoon representation of the NanoBRET strategy to detect binding to the IABS of CCR6. B) Specific saturation binding curves of fluorescent tracers 3–5 in a NanoBRET-based assay using CCR6\_Nluc membranes (mean  $\pm$  SEM, triplicate measurement,  $n = 3$ ). C) Overlay of the predicted CCR6 (purple) binding mode 5 (green) with the observed CXCR2 (grey) binding mode of 00767013 (7, cyan, PDB ID: 6LFL).<sup>[6]</sup> D) Kinetic binding studies at room temperature. Representative association and dissociation curves with 5 (50 nM) using CCR6\_Nluc membranes ( $n = 4$  association,  $n = 3$  for dissociation). E) Competition binding curves and detected  $pK_i$  values (mean  $\pm$  SEM, triplicate measurement,  $n \geq 3$ ) for the known CXCR1/CXCR2 antagonist navarixin (1),<sup>[18b]</sup> the linker-ligand conjugate (6),<sup>[8b]</sup> and the extracellular orthosteric CCR6 agonist CCL20<sup>[20]</sup> obtained with 5 (250 nM) and CCR6\_Nluc membranes.  $K_i$  values are given in square brackets. F) Z'-factor determination for the cell-free NanoBRET-based setup using 5 (250 nM) and CCR6\_Nluc membranes (36-fold determination). G) Saturation binding curve of 5 in a cellular NanoBRET-based experiment (mean  $\pm$  SEM, triplicate measurement,  $n = 3$ ) using live HEK293T cells transiently expressing CCR6\_GSSG\_Nluc. H) Cellular competition binding curve and  $pK_i$  value (mean  $\pm$  SEM, quadruplicate measurement,  $n = 3$ ) for 1 obtained with 5 (250 nM) and live HEK293T cells transiently expressing CCR6\_GSSG\_Nluc.  $K_i$  value is given in square brackets.

For our membrane-based CCR6 competition binding assay, we determined a Z'-factor of 0.83, which highlights the high quality of 5 as a fluorescent tracer for cell-free CCR6 binding studies and its suitability for HTS approaches.

For our cell-based binding assay, we used live HEK293T cells transiently expressing CCR6\_GSSG\_Nluc, as this construct resulted in a larger and more robust assay window compared to CCR6\_Nluc under cellular conditions (Figure S4A). Using this setup, we detected a  $K_D$  value of  $32.5 \pm 9.5$  nM (Figures 3G and S4B). This is highly consistent with the equilibrium  $K_D$  detected under cell-free conditions ( $K_D = 38.0$  nM), thus indicating that 5 is also able to bind to the IABS of CCR6 in a cellular environment. However, the low delta-BRET ( $\sim 0.05$ ) of our cell-based CCR6 binding assay resulted in relatively high standard errors of the individual measuring points and the derived  $K_D$  value (Figures 3G and S4C). A similar behaviour was observed when using 5 as a tracer for cellular competition binding studies. For the reference ligand 1, our cellular competition binding assay allowed the detection of a CCR6 affinity ( $pK_i = 6.17 \pm 0.07$  [700 nM], Figure 3H), which is in good agreement with the  $K_i$  detected under cell-free conditions. However, the relatively large error bars that can be observed in the individual triplicate measurements (Figure S4D) indicate the limitations of a cellular application of 5 as a tracer for CCR6. Nevertheless, taking into account these limitations, 5 is a very valuable tool for a first assessment of cellular target engagement for the IABS of CCR6.

### Mapping of Binding Sites of Previously Reported CXCR1 and/or CCR6 Ligands

After having demonstrated the suitability of LT221 (5) as a fluorescent tracer to detect binding to the IABS of CXCR1 and CCR6, we aimed for using our new membrane-based binding assays to study which of the previously reported CXCR1 and/or CCR6 ligands are binding to the IABS of their target receptor and which are binding to different binding sites. For CXCR1, we selected the previously reported diarylurea-based CXCR2 antagonists danirixin (8)<sup>[25]</sup> and SB225002 (9),<sup>[26]</sup> which are known to show at least some off-target affinity for CXCR1, the squaramide-based dual CXCR1/CXCR2 antagonist cmpd24 (10),<sup>[18b]</sup> and the highly selective dual CXCR1/CXCR2 antagonist reparixin (11, Figure 4A).<sup>[27]</sup> As CCR6 ligands we chose the CCR6 antagonist 1 (12),<sup>[18e]</sup> CCR6 inhibitor 1 (13),<sup>[28]</sup> and the squaramide PF-07054894 (2, Figure 4A).<sup>[18d]</sup> In a first run we screened the compounds for competition with 5 (250 nM) at a concentration of 10  $\mu$ M. As reference compounds we included 1 and 6, which were already used during the development of our CXCR1 and CCR6 assays, respectively.

Among the known CXCR1 ligands, the squaramide-based 10<sup>[18b]</sup> as well as the diarylurea 8<sup>[25]</sup> showed strong competition with 5 for intracellular CXCR1 binding (Figure 4B). This is not surprising because both compounds feature sub-micromolar potencies for CXCR1 and both squaramides and diarylureas are chemotypes that were previously reported to bind to the IABS

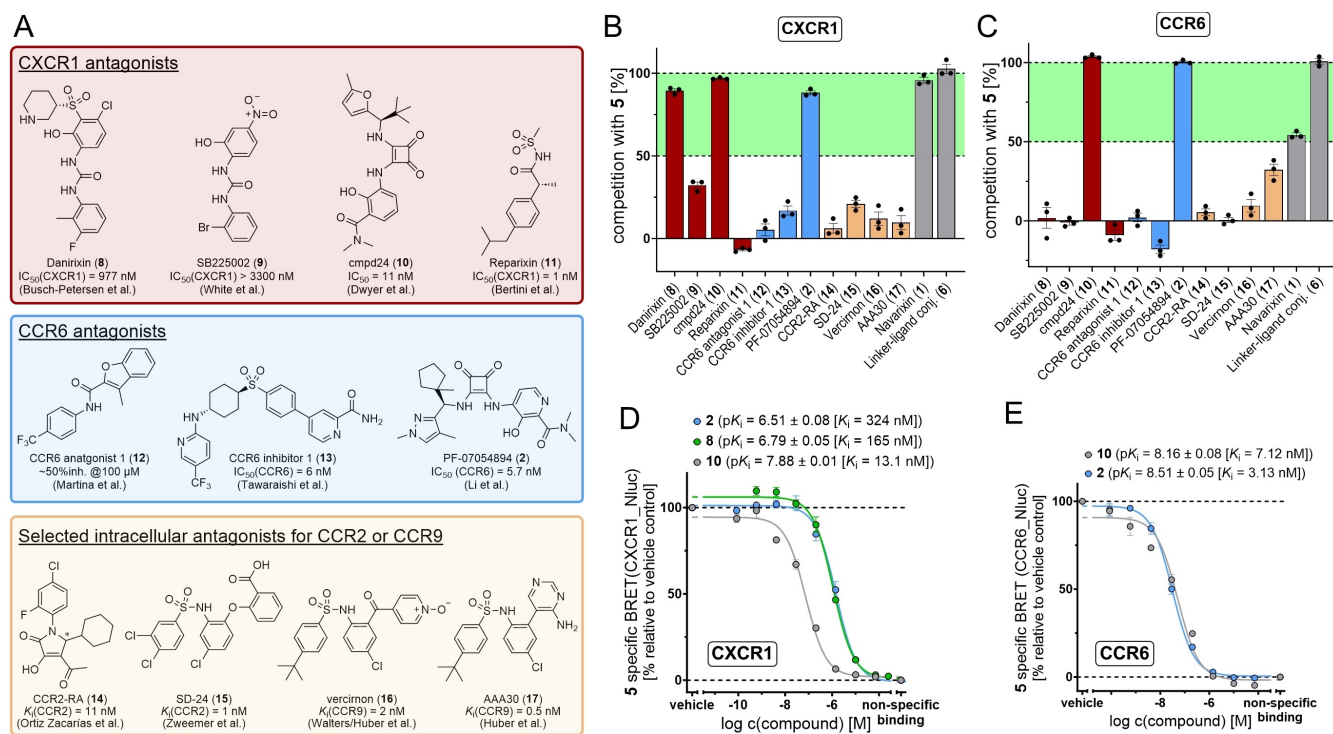


**Figure 4.** Application of LT221 (5) as a fluorescent tool for mapping binding sites of known and potential CXCR1 and/or CCR6 ligands. A) Chemical structures and reported biological data of known chemokine receptor ligands 8–17.<sup>[8a,15,18b,d,25–28,30]</sup> B) Competition of known chemokine receptor ligands 8–17 (10 μM) with 5 (250 nM) for binding to the IABS of CXCR1 (mean ± SEM, quadruplicate measurement, n = 3). NanoBRET-based competition binding studies were performed with CXCR1\_Nluc membranes. C) Competition of known chemokine receptor ligands 8–17 (10 μM) with 5 (250 nM) for binding to the IABS of CCR6 (mean ± SEM, quadruplicate measurement, n = 3). NanoBRET-based competition binding studies were performed with CCR6\_Nluc membranes. D) Competition binding curves and detected pK<sub>i</sub> values (mean ± SEM, triplicate measurement, n = 3) for identified intracellular CXCR1 binders. Tests were performed with CXCR1\_Nluc membranes. E) Competition binding curves and detected pK<sub>i</sub> values (mean ± SEM, triplicate measurement, n = 3) for identified intracellular CCR6 binders. Tests were performed with CCR6\_Nluc membranes.

of the closely related CXCR2.<sup>[8b,18b,25]</sup> Docking studies suggested that the diarylureas gain their CXCR1 affinity by forming a bifurcated H-bond interaction with D75<sup>2x40</sup> (Figure S5A), in a highly similar manner as observed for the squaramides 1 and 6 (Figure 2C). For the diarylurea 9,<sup>[26]</sup> we detected a weaker binding to the IABS of CXCR1, which is consistent with its weaker CXCR1 potency compared to the structurally similar 8. The high-affinity dual CXCR1/CXCR2 antagonist 11 showed no competition with 5, which is in good agreement with reports suggesting an extracellular allosteric binding site for this compound.<sup>[27,29]</sup>

Of the selected known CCR6 ligands, 12<sup>[18e]</sup> and 13<sup>[28]</sup> showed no competition with 5 for intracellular CCR6 binding, thereby indicating different binding sites than the IABS for these ligands (Figure 4C). These observations are consistent with an extracellular binding mode of both compounds that has been suggested by Martina *et al.* based on docking studies.<sup>[18e]</sup> For the highly potent CCR6 antagonist 2,<sup>[18d]</sup> currently in phase I clinical trials for ulcerative colitis, we detected a very strong competition, thus clearly indicating binding to the IABS of CCR6. This finding is in full agreement with i) an insurmountable inhibition mode of 2 regarding CCL20/CCR6-mediated T-cell chemotaxis, as reported by Li *et al.*,<sup>[18d]</sup> and ii) the fact that squaramide-based compounds are well known intracellular chemokine receptor ligands.<sup>[6,12b]</sup>

Since our initial tests indicated that there is a certain overlap between intracellular CXCR1 and CCR6 ligands, especially among the squaramides, we tested the known CXCR1 ligands at CCR6 and *vice versa* (Figure 4B–C). Here, we detected that the CCR6-targeted 2 also binds to CXCR1 and that the dual CXCR1/CXCR2 antagonist 10 seems to feature a significant affinity for CCR6.

In order to provide initial insights into the promiscuity of the intracellular allosteric binding sites of CXCR1 and CCR6, we tested selected intracellular allosteric antagonists of other chemokine receptors for their competition with 5 (Figure 4A). These ligands, including the CCR2-targeted CCR2-RA (14),<sup>[8a]</sup> and SD-24 (15),<sup>[30b,31]</sup> the CCR9-targeted verciron (16),<sup>[15,30a]</sup> and AAA30 (17),<sup>[15]</sup> which were all reported as antagonists with sub-nanomolar to low-nanomolar affinities for their targeted receptor, showed strongly reduced binding to CXCR1 and CCR6. This highlights the low promiscuity of these ligands and further indicates that the IABSs of both CXCR1 and CCR6 are not promiscuous as well, thus corroborating their potential as drug target sites for the development of selective drugs.

The ligands that showed greater than 50% inhibition at a concentration of 10 μM in the initial tests with CXCR1 or CCR6 were further characterized. Concentration dependent competition binding studies resulted in CXCR1 affinities of pK<sub>i</sub> = 7.88 ± 0.01 [13.1 nM] for 10, pK<sub>i</sub> = 6.79 ± 0.05 [165 nM] for 8, and pK<sub>i</sub> =

$6.51 \pm 0.08$  [324 nM] for **2** (Figures 4D and S5B). In analogous tests with CCR6, we detected affinities of  $pK_i = 8.16 \pm 0.08$  [7.12 nM] for **10**, and  $pK_i = 8.51 \pm 0.05$  [3.13 nM] for **2** (Figures 4E and S5C). The observed affinity of **2** to the IABS of CCR6 is highly consistent with the reported  $IC_{50}$  value of 5.7 nM,<sup>[18d]</sup> which further corroborates an intracellular CCR6 binding mode of this compound.

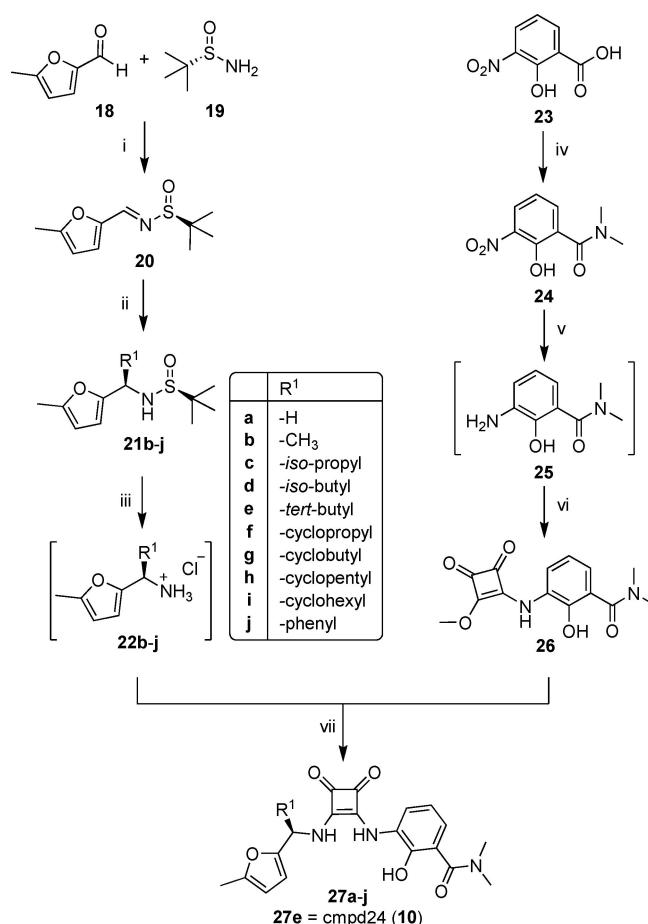
### SAR Study for Squaramide-Based CCR6/CXCR1 Ligands

Intrigued by the approximately 150-fold gain in CCR6 affinity by replacing the ethyl substituent at the chiral carbon atom of **1** with a *tert*-butyl group, as found in **10**, we aimed for systematically studying the SAR of this highly important position by using our newly established assay platform. Therefore, we synthesized and tested several analogues of **1** that differ in their substituents at this position. As substituents we considered linear, branched, and cyclic alkyl moieties as well as phenyl as an aromatic group. For the synthesis of these compounds, we adapted our previously reported procedure for the synthesis of CXCR2-targeted fluorescent probes (Scheme 1).<sup>[8b]</sup> Combining the screening platform for CXCR1 and CCR6, as described above, with our previously reported CXCR2 assay,<sup>[8b]</sup> we investigated CXCR1/CXCR2/CCR6 selectivity profiles of the synthesized navarixin analogues **27 a–j** (Table 1).

Regarding CCR6 affinity, we identified the *tert*-butyl moiety as an absolute sweet spot. By means of docking experiments we were able to rationalize the massive effect of the *tert*-butyl group on CCR6 affinity, which is mediated *via* hydrophobic interactions with an aromatic cage that is formed by F71<sup>1×57</sup>, Y316<sup>7×53</sup>, F323<sup>8×50</sup>, and Y326<sup>8×53</sup> (Figure 5A, and S6A). This aromatic cage is a special feature of CCR6 and not present in CXCR1 or CXCR2, due to their lack of an aromatic amino acid in positions 1×57 and 8×53 (Figure S6B). Smaller and less bulky residues like a proton (**27 a**), methyl (**27 b**), or ethyl (**1**) can hardly build up the hydrophobic interactions that are required to anchor the ligand in this aromatic cage. The same seems to be the case for flat aliphatic residues such as cyclopropyl (**27 f**) and cyclobutyl (**27 g**). The branched aliphatic groups like *iso*-propyl (**27 c**), *iso*-butyl (**27 d**), as well as cyclopentyl (**27 h**), which predominantly exists in an envelope conformation, can at least address the hydrophobic interactions with the aromatic cage to some extent. The aliphatic or aromatic six-membered rings (i.e., cyclohexyl (**27 i**) and phenyl (**27 j**)), seem to penetrate too deep into the binding pocket, which might result in a steric clash, thus explaining the strongly reduced CCR6 affinities of these ligands.

In the case of CXCR1 and CXCR2, a *tert*-butyl substituent is well tolerated, as indicated by the detected affinities of **10**, but not essential, as highlighted by similar CXCR1 or CXCR2 affinities of the ethyl (**1**) and *iso*-propyl (**27 c**) analogues. Nonetheless, a certain degree of hydrophobicity at this position is also required for CXCR1 and CXCR2 binding, which is shown by the activity cliff when moving from ethyl (**1**) to methyl (**27 a**).

Overall, our SAR data underlines the utmost importance of a bulky hydrophobic substituent at the chiral carbon atom of the



**Scheme 1.** Synthesis of analogues of **cmpd24** (**10**). Reagents and conditions: i)  $Ti(OEt)_4$ ,  $Na_2SO_4$ ,  $CH_2Cl_2$ , rt, overnight, quantitative yield. ii) for **21 b–e** and **21 h–j**: Respective alkyl- or arylmagnesium chloride, THF, 0 °C to rt, 3 d, 13–54% yield; for **21 f–g**: Mg,  $I_2$ , alkyl bromide, THF, 50 °C, 30 min; then **20**, THF, 0 °C to rt, 3 d, 14–17% yield. iii) HCl (in  $Et_2O$ ), MeOH, 0 °C to rt, 1 h (crude). iv) oxalyl chloride, DMF (cat.),  $CH_2Cl_2$ , rt, overnight; then, dimethyl amine, DIPEA,  $CH_2Cl_2$ , 0 °C to rt, overnight, 26% yield. v)  $H_2$ , Pd/C, EtOH, rt, overnight (crude). vi) dimethyl squarate, MeOH, rt, overnight, 93% yield. vii) for **27 a**: (5-methylfuran-2-yl)methanamine (**22 a**), **26**, DIPEA, MeOH, 3 d, 21% yield; for **27 b–j**: hydrochloride salt of the respective amine (**22 b–j**), **26**, DIPEA, MeOH, rt, 3 d, 10–49% yield. For clarity, only the major diastereomers and enantiomers, respectively, are shown. Detailed information on diastereomeric purities of compounds **21 b–j** is provided in the Supporting Information.

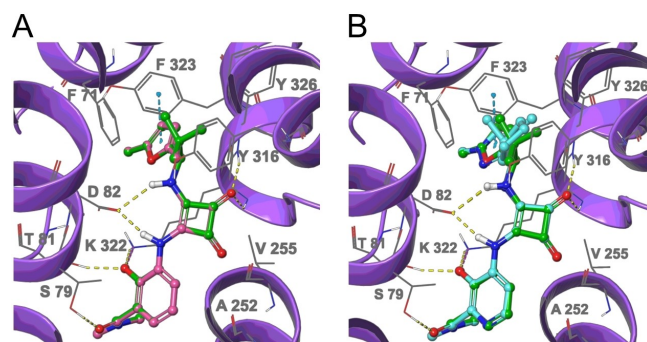


**Figure 5.** Predicted binding modes of small molecule antagonists to the IABS of CCR6 (purple). A) Overlay of the predicted binding modes of **10** (green) and **1** (magenta). The *tert*-butyl moiety of **10** anchors the ligand to the IABS of CCR6 via hydrophobic interactions with an aromatic cage. B) Overlay of the predicted binding modes of **10** (green) and **2** (cyan), suggests highly similar binding modes to the IABS of CCR6.



**Table 1.** SAR study for analogues of the squaramide-based ligand cmpd24 (**10**). Table shows CCR6, CXCR1, and CCR9 affinity data for **10** and its analogues **27a–d** and **27f–j**. **1** and the linker-ligand conjugate **6** were used as reference compounds. CCR6 and CXCR1 affinity data was obtained by means of our cell-free NanoBRET competition binding assays using **5** (250 nM) and CCR6\_Nluc or CXCR1\_Nluc membranes. CXCR2 affinity data was obtained by using a cell-free NanoBRET competition binding assay as previously reported.<sup>[8b]</sup> Experiments were performed in triplicate ( $n \geq 3$ ).

	R <sup>1</sup>	R <sup>2</sup>	R <sup>3</sup>	pK <sub>i</sub> ± SEM (K <sub>i</sub> [nM]) or comp.		
				CCR6	CXCR1	CXCR2
<b>6</b>	-H		- <i>tert</i> -butyl	7.99 ± 0.01 (10.1)	7.78 ± 0.07 (17.3)	9.37 ± 0.03 (0.43)
<b>27a</b>	-CH <sub>3</sub>	-CH <sub>3</sub>	-H	-3% comp. @10 μM	9% comp. @10 μM	7.30 ± 0.02 (50.0)
<b>27b</b>	-CH <sub>3</sub>	-CH <sub>3</sub>	-CH <sub>3</sub>	5.31 ± 0.02 (4930)	5.60 ± 0.08 (2580)	7.09 ± 0.01 (81.8)
navarixin ( <b>1</b> )	-CH <sub>3</sub>	-CH <sub>3</sub>	-CH <sub>2</sub> -CH <sub>3</sub>	5.98 ± 0.02 (1060)	7.64 ± 0.06 (23.6)	10.23 ± 0.07 (0.06)
<b>27c</b>	-CH <sub>3</sub>	-CH <sub>3</sub>	- <i>iso</i> -propyl	7.17 ± 0.08 (70.3)	7.87 ± 0.06 (13.8)	9.87 ± 0.05 (0.14)
<b>27d</b>	-CH <sub>3</sub>	-CH <sub>3</sub>	- <i>iso</i> -butyl	6.31 ± 0.04 (494)	6.82 ± 0.04 (154)	8.75 ± 0.05 (1.82)
cmpd24 ( <b>10</b> )	-CH <sub>3</sub>	-CH <sub>3</sub>	- <i>tert</i> -butyl	8.16 ± 0.08 (7.12)	7.88 ± 0.01 (13.1)	10.05 ± 0.07 (0.09)
<b>27f</b>	-CH <sub>3</sub>	-CH <sub>3</sub>	-cyclopropyl	5.84 ± 0.03 (1440)	6.69 ± 0.06 (211)	8.29 ± 0.03 (5.11)
<b>27g</b>	-CH <sub>3</sub>	-CH <sub>3</sub>	-cyclobutyl	6.00 ± 0.03 (994)	7.15 ± 0.02 (71.6)	8.52 ± 0.01 (3.02)
<b>27h</b>	-CH <sub>3</sub>	-CH <sub>3</sub>	-cyclopentyl	7.01 ± 0.02 (99.2)	7.05 ± 0.03 (89.3)	9.03 ± 0.04 (0.94)
<b>27i</b>	-CH <sub>3</sub>	-CH <sub>3</sub>	-cyclohexyl	5.87 ± 0.08 (1410)	6.14 ± 0.05 (741)	7.63 ± 0.07 (23.8)
<b>27j</b>	-CH <sub>3</sub>	-CH <sub>3</sub>	-phenyl	5.73 ± 0.09 (1960)	6.10 ± 0.01 (789)	7.85 ± 0.08 (14.5)

navarixin-based scaffold for CCR6 affinity. This is also reflected by the structure of the clinical candidate **2**, which features a bulky 1-methylcyclopentyl residue at this important position. Our docking studies indicated that this moiety of **2** interacts with the aromatic cage in a very similar manner to that predicted for the *tert*-butyl group of **10** (Figure 5B).

### Cellular Characterization of **10** as a CCR6 Antagonist

To investigate if the low nanomolar CCR6 affinity of **10**, which was detected under cell-free conditions, also translates into cellular affinity and finally cellular activity, we first used our cell-based NanoBRET competition binding assay. Taking into account the aforementioned limitations of our cellular CCR6 binding assay, we detected a cellular CCR6 affinity of  $pK_i = 7.95 \pm 0.02$  [11.2 nM] (Figures 6A and S7A), which is consistent with the  $K_i$  detected under cell-free conditions ( $K_i = 7.12$  nM). This initial estimation of cellular CCR6 affinity was confirmed by a cellular NanoBiT-based  $\beta$ -arrestin-2 recruitment assay. Here, **10** evoked an inhibition of CCL20 induced  $\beta$ -arrestin-2 recruitment with a  $pIC_{50}$  value of  $7.94 \pm 0.08$  [11.4 nM] (Figure 6B), thereby underlining that the low nanomolar CCR6 affinity detected under cell-free and cell-based condition results in a highly potent inhibition of CCR6's activity. In our cellular CXCR1 competition binding assay, we also detected a low nanomolar affinity of **10**,  $8.46 \pm 0.09$  [ $K_i = 3.9$  nM], for CXCR1 (Figure S7B–C).

## Conclusions

In summary, starting from the previously reported fluorescent ligand LT221 (**5**) targeting the intracellular allosteric binding site (IABS) of the chemokine receptor CXCR2, we developed a NanoBRET-based assay platform to detect intracellular binding to CCR6 and CXCR1. These two chemokine receptors are

promising drug targets in inflammation and immuno-oncology. Our assay platform enabled cell-free as well as cellular NanoBRET-based binding studies in a nonisotopic and straightforward manner. By means of this assay platform, we: i) provided evidence for the existence of a druggable IABS at CCR6 and CXCR1; ii) mapped known CXCR1 or CCR6 antagonists, such as the current clinical candidate and high affinity CCR6 antagonist PF-07054894 (**2**), to the IABS of their target receptor; and iii) established a SAR model for squaramide-based antagonists highlighting the importance of hydrophobic ligand interactions with an aromatic cage, which is a special feature of the IABS of CCR6. In the course of our SAR studies, we identified the squaramide **10** as an intracellular CCR6 antagonist with single-digit nanomolar affinity and low nanomolar potency ( $IC_{50} = 11.4$  nM) for CCL20-induced receptor activation. The high affinity of this compound was rationalized by strong hydrophobic interaction of its *tert*-butyl moiety with the aromatic

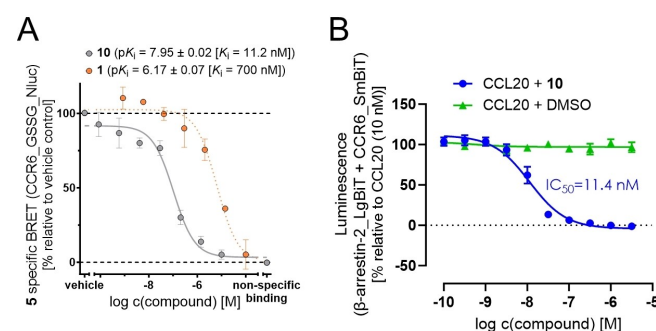


**Figure 6.** Cellular evaluation of **10** as an intracellular CCR6 antagonist. A) Cellular competition binding curve and  $pK_i$  value (mean ± SEM, quadruplicate measurement,  $n = 3$ ) for **10** (grey) obtained with **5** (250 nM) and live HEK293T cells transiently expressing CCR6\_GSSG\_Nluc.  $K_i$  values are given in square brackets. The competition binding curve of **1** (dashed orange line) is shown for comparison. B) Concentration-response curve of **10** in a cellular NanoBiT-based  $\beta$ -arrestin-2 recruitment assay ( $n \geq 3$ , see Experimental Section for more details).



cage of CCR6. Of course, this compound cannot be considered as a CCR6 selective probe, due to its high affinity binding to CXCR1 and especially CXCR2. Nonetheless, **10** represents a highly valuable tool compound for studying the effects of intracellular CCR6 inhibition in test systems where only CCR6 is overexpressed.

Overall, we showed that our newly developed NanoBRET assays form a highly valuable platform that will leverage the discovery of future drug candidates binding to the intracellular allosteric binding sites of CXCR1 and CCR6.

## Supporting Information

The Supporting Information is available via <https://doi.org/10.1002/cmdc.202400284> and includes experimental details for compound synthesis, biological tests, and molecular docking, Supplementary Figures S1–S7, as well as NMR spectra and HPLC traces for all final compounds. The authors have cited additional references within the Supporting Information.<sup>[32]</sup>

## Acknowledgements

M. S. (Li 204/04) was supported by the Verband der Chemischen Industrie (VCI). A. C., M. S., and A. A. B. were supported by the Luxembourg Institute of Health (LIH) through the NanoLux Platform, the Luxembourg National Research Fund (INTER/FNRS grants INTER 20/15084569, CORE C23/BM/18068832, and PRIDE-16749720 “NextImmune2”). Further, we thank Prof. Peter Gmeiner for mentoring and hosting the research of M. S. The authors thank Theresa Pröll for supporting the preparation of Figures 2A and 3A, which were created with BioRender.com. Further, the authors would like to thank Nadia Beaupain and Manuel Counson for technical support. Open Access funding enabled and organized by Projekt DEAL.

## Conflict of Interests

The authors declare no conflict of interest.

## Data Availability Statement

The data that support the findings of this study are available in the supplementary material of this article.

**Keywords:** GPCRs • Allosteric modulators • Drug discovery • NanoBRET • Medicinal Chemistry

- [1] R. Santos, O. Ursu, A. Gaulton, A. P. Bento, R. S. Donadi, C. G. Bologa, A. Karlsson, B. Al-Lazikani, A. Hersey, T. I. Oprea, J. P. Overington, *Nat. Rev. Drug Discovery* **2017**, *16*, 19–34.  
[2] J. B. Hedderich, M. Persechino, K. Becker, F. M. Heydenreich, T. Gutermuth, M. Bouvier, M. Bünemann, P. Kolb, *Nat. Commun.* **2022**, *13*, 2567.

- [3] Y. Zheng, L. Qin, N. V. Zacarias, H. de Vries, G. W. Han, M. Gustavsson, M. Dabros, C. Zhao, R. J. Cherney, P. Carter, D. Stamos, R. Abagyan, V. Cherezov, R. C. Stevens, A. P. IJzerman, L. H. Heitman, A. Tebben, I. Kufareva, T. M. Handel, *Nature* **2016**, *540*, 458–461.  
[4] K. Jaeger, S. Bruenle, T. Weinert, W. Guba, J. Muehle, T. Miyazaki, M. Weber, A. Furrer, N. Haenggi, T. Tetaz, C. Y. Huang, D. Mattle, J. M. Vonach, A. Gast, A. Kuglstatter, M. G. Rudolph, P. Nogly, J. Benz, R. J. P. Dawson, J. Standfuss, *Cell* **2019**, *178*, 1222–1230.  
[5] C. Oswald, M. Rappas, J. Kean, A. S. Dore, J. C. Errey, K. Bennett, F. Deflorian, J. A. Christopher, A. Jazayeri, J. S. Mason, M. Congreve, R. M. Cooke, F. H. Marshall, *Nature* **2016**, *540*, 462–465.  
[6] K. Liu, L. Wu, S. Yuan, M. Wu, Y. Xu, Q. Sun, S. Li, S. Zhao, T. Hua, Z. J. Liu, *Nature* **2020**, *585*, 135–140.  
[7] X. Liu, S. Ahn, A. W. Kahsai, K. C. Meng, N. R. Latorraca, B. Pani, A. J. Venkatakrishnan, A. Masoudi, W. I. Weis, R. O. Dror, X. Chen, R. J. Lefkowitz, B. K. Kobilka, *Nature* **2017**, *548*, 480–484.  
[8] a) N. V. Ortiz Zacarias, J. P. D. van Veldhoven, L. Portner, E. van Spronsen, S. Ullo, M. Veenhuizen, W. J. C. van der Velden, A. J. M. Zweemer, R. M. Kreekel, K. Oenema, E. B. Lenselink, L. H. Heitman, A. P. IJzerman, *J. Med. Chem.* **2018**, *61*, 9146–9161; b) M. E. Huber, S. Wurnig, L. Toy, C. Weiler, N. Merten, E. Kostenis, F. K. Hansen, M. Schiedel, *J. Med. Chem.* **2023**, *66*, 9916–9933.  
[9] R. Solari, J. E. Pease, M. Begg, *Eur. J. Pharmacol.* **2015**, *746*, 363–367.  
[10] a) A. J. Armstrong, R. Geva, H. C. Chung, C. Lemeck, W. H. Miller Jr., A. R. Hansen, J. S. Lee, F. Tsai, B. J. Solomon, T. M. Kim, C. Rolfo, V. Giranda, Y. Ren, F. Liu, B. Kandala, T. Freshwater, J. S. Wang, *Invest. New Drugs* **2024**, *42*, 145–159; b) M. Billen, D. Schols, P. Verwilst, *Chem. Commun.* **2022**, *58*, 4132–4148.  
[11] a) C. W. Lindsley, K. A. Emmitte, C. R. Hopkins, T. M. Bridges, K. J. Gregory, C. M. Niswender, P. J. Conn, *Chem. Rev.* **2016**, *116*, 6707–6741; b) N. T. Burford, J. Watson, R. Bertekap, A. Alt, *Biochem. Pharmacol.* **2011**, *81*, 691–702.  
[12] a) A. J. Zweemer, I. Nederpelt, H. Vrieling, S. Hafith, M. L. Doornbos, H. de Vries, J. Abt, R. Gross, D. Stamos, J. Saunders, M. J. Smit, A. P. IJzerman, L. H. Heitman, *Mol. Pharmacol.* **2013**, *84*, 551–561; b) K. Salchow, M. E. Bond, S. C. Evans, N. J. Press, S. J. Charlton, P. A. Hunt, M. E. Bradley, *Br. J. Pharmacol.* **2010**, *159*, 1429–1439.  
[13] a) M. E. Huber, L. Toy, M. F. Schmidt, D. Weikert, M. Schiedel, *Chem. Eur. J.* **2023**, *29*, e202202565; b) J. Gleixner, S. Kopanchuk, L. Gratz, M. J. Tahk, T. Laasfeld, S. Veiksina, C. Höring, A. O. Gattor, L. J. Humphrys, C. Müller, N. Archipowa, J. Köckenberger, M. R. Heinrich, R. J. Kutta, A. Rinken, M. Keller, *ACS Pharmacol. Transl. Sci.* **2024**, *7*, 1142–1168.  
[14] L. Toy, M. E. Huber, M. F. Schmidt, D. Weikert, M. Schiedel, *ACS Chem. Biol.* **2022**, *17*, 2142–2152.  
[15] M. E. Huber, L. Toy, M. F. Schmidt, H. Vogt, J. Budzinski, M. F. J. Wiefhoff, N. Merten, E. Kostenis, D. Weikert, M. Schiedel, *Angew. Chem. Int. Ed.* **2022**, *61*, e202116782.  
[16] B. M. Casella, J. P. Farmer, D. N. Nesheva, H. E. L. Williams, S. J. Charlton, N. D. Holliday, C. A. Laughton, S. N. Mistry, *J. Med. Chem.* **2023**, *66*, 12911–12930.  
[17] a) T. Machleidt, C. C. Woodroffe, M. K. Schwinn, J. Mendez, M. B. Robers, K. Zimmerman, P. Otto, D. L. Daniels, T. A. Kirkland, K. V. Wood, *ACS Chem. Biol.* **2015**, *10*, 1797–1804; b) L. A. Stoddart, L. E. Kilpatrick, S. J. Hill, *Trends Pharmacol. Sci.* **2018**, *39*, 136–147.  
[18] a) J. Che, R. Song, B. Chen, X. Dong, *Eur. J. Med. Chem.* **2020**, *185*, 111853; b) M. P. Dwyer, Y. Yu, J. Chao, C. Aki, J. Chao, P. Biju, V. Girijavallabhan, D. Rindgen, R. Bond, R. Mayer-Ezel, J. Jakway, R. W. Hipkin, J. Fossetta, W. Gonsiorek, H. Bian, X. Fan, C. Terminelli, J. Fine, D. Lundell, J. R. Merritt, L. L. Rokosz, B. Kaiser, G. Li, W. Wang, T. Stauffer, L. Ozgur, J. Baldwin, A. G. Taveras, *J. Med. Chem.* **2006**, *49*, 7603–7606; c) W. Gonsiorek, X. D. Fan, D. Hesk, J. Fossetta, H. C. Qiu, J. Jakway, M. Billah, M. Dwyer, J. H. Chao, G. Deno, A. Taveras, D. J. Lundell, R. W. Hipkin, *J. Pharmacol. Exp. Ther.* **2007**, *322*, 477–485; d) W. Li, K. K. Crouse, J. Alley, R. K. Frisbie, S. C. Fish, T. A. Andreyeva, L. A. Reed, M. Thorn, G. DiMaggio, C. B. Donovan, D. Bennett, J. Garren, E. Oziolor, J. Qian, L. Newman, A. P. Vargas, S. W. Kumpf, S. J. Steyn, M. E. Schnute, A. Thorarensen, M. Hegen, E. Stevens, M. Collinge, T. A. Lanz, F. Vincent, M. S. Vincent, G. Berstein, *J. Pharmacol. Exp. Ther.* **2023**, *386*, 80–92; e) M. G. Martina, C. Giorgio, M. Alodi, S. Palese, E. Barocelli, V. Ballabeni, M. Szpakowska, A. Chevigne, J. Piet van Hamburg, N. Davelaar, E. Lubberts, S. Bertoni, M. Radi, *Eur. J. Med. Chem.* **2022**, *243*, 114703.  
[19] B. S. Gerstenberger, A. C. Flick, V. M. Lombardo, J. J. Mousseau, P. M. Nuhant, R. P. Robinson Jr, M. E. Schnute, D. W.-S. Kung, D. C. Schmitt, A. Thorarensen, J. I. Trujillo, R. J. Unwalla, H. Wu, N-substituted-dioxocyclo-

- butenylamino-3-hydroxy-picolinamides usefull as CCR6 inhibitors. US 10,975,065 B2, 2021.
- [20] a) D. A. Hall, I. J. Beresford, C. Browning, H. Giles, *Br. J. Pharmacol.* **1999**, 126, 810–818; b) S. Wilson, G. Wilkinson, G. Milligan, *J. Biol. Chem.* **2005**, 280, 28663–28674.
- [21] H. Vogt, P. Shinkwin, M. E. Huber, N. Staffen, H. Hübner, P. Gmeiner, M. Schiedel, D. Weikert, *ACS Pharmacol. Transl. Sci.* **2024**, 7, 1533–1545.
- [22] J. H. Zhang, T. D. Chung, K. R. Oldenburg, *J. Biomol. Screening* **1999**, 4, 67–73.
- [23] J. Stefaniak, K. V. M. Huber, *ACS Med. Chem. Lett.* **2020**, 11, 403–406.
- [24] D. R. Greaves, W. Wang, D. J. Dairaghi, M. C. Dieu, B. Saint-Vis, K. Franz-Bacon, D. Rossi, C. Caux, T. McClanahan, S. Gordon, A. Zlotnik, T. J. Schall, *J. Exp. Med.* **1997**, 186, 837–844.
- [25] J. Busch-Petersen, D. C. Carpenter, M. Burman, J. Foley, G. E. Hunsberger, D. J. Kilian, M. Salmon, R. J. Mayer, J. G. Yonchuk, R. Tal-Singer, *J. Pharmacol. Exp. Ther.* **2017**, 362, 338–346.
- [26] J. R. White, J. M. Lee, P. R. Young, R. P. Hertzberg, A. J. Jurewicz, M. A. Chaikin, K. Widdowson, J. J. Foley, L. D. Martin, D. E. Griswold, H. M. Sarau, *J. Biol. Chem.* **1998**, 273, 10095–10098.
- [27] R. Bertini, M. Allegretti, C. Bizzarri, A. Moriconi, M. Locati, G. Zampella, M. N. Cervellera, V. Di Cioccio, M. C. Cesta, E. Galliera, F. O. Martinez, R. Di Bitondo, G. Troiani, V. Sabbatini, G. D'Anniballe, R. Anacardio, J. C. Cutrin, B. Cavalieri, F. Mainiero, R. Strippoli, P. Villa, M. Di Girolamo, F. Martin, M. Gentile, A. Santoni, D. Corda, G. Poli, A. Mantovani, P. Ghezzi, F. Colotta, *Proc. Natl. Acad. Sci. USA* **2004**, 101, 11791–11796.
- [28] T. Tawaraishi, N. Sakauchi, K. Hidaka, K. Yoshikawa, T. Okui, H. Kuno, I. Chisaki, K. Aso, *Bioorg. Med. Chem. Lett.* **2018**, 28, 3067–3072.
- [29] R. Bertini, L. S. Barcelos, A. R. Beccari, B. Cavalieri, A. Moriconi, C. Bizzarri, P. Di Benedetto, C. Di Giacinto, I. Gloaguen, E. Galliera, M. M. Corsi, R. C. Russo, S. P. Andrade, M. C. Cesta, G. Nano, A. Aramini, J. C. Cutrin, M. Locati, M. Allegretti, M. M. Teixeira, *Br. J. Pharmacol.* **2012**, 165, 436–454.
- [30] a) M. J. Walters, Y. Wang, N. Lai, T. Baumgart, B. N. Zhao, D. J. Dairaghi, P. Bekker, L. S. Ertl, M. E. Penfold, J. C. Jaen, S. Keshav, E. Wendt, A. Pennell, S. Ungashe, Z. Wei, J. J. Wright, T. J. Schall, *J. Pharmacol. Exp. Ther.* **2010**, 335, 61–69; b) A. J. M. Zweemer, J. Bunnik, M. Veenhuizen, F. Miraglia, E. B. Lenselink, M. Vilums, H. de Vries, A. Gibert, S. Thiele, M. M. Rosenkilde, A. P. IJzerman, L. H. Heitman, *Mol. Pharmacol.* **2014**, 86, 358–368.
- [31] S. Peace, J. Philp, C. Brooks, V. Piercy, K. Moores, C. Smethurst, S. Watson, S. Gaines, M. Zippoli, C. Mookherjee, R. Ife, *Bioorg. Med. Chem. Lett.* **2010**, 20, 3961–3964.
- [32] a) A. S. Hashmi, T. Haffner, W. Yang, S. Pankajakshan, S. Schafer, L. Schultes, F. Rominger, W. Frey, *Chem. Eur. J.* **2012**, 18, 10480–10486; b) A. S. K. Hashmi, S. Schäfer, J. W. Bats, W. Frey, F. Rominger, *Eur. J. Org. Chem.* **2008**, 2008, 4891–4899; c) J. R. Merritt, L. L. Rokosz, K. H. Nelson Jr., B. Kaiser, W. Wang, T. M. Stauffer, L. E. Ozgur, A. Schilling, G. Li, J. J. Baldwin, A. G. Taveras, M. P. Dwyer, J. Chao, *Bioorg. Med. Chem. Lett.* **2006**, 16, 4107–4110; d) A. G. Taveras, C. J. Aki, J. Chao, M. Dwyer, J. Chao, Y. Yu, J. R. Merritt, P. Biju, J. Jakway, G. Lai, M. Wu, E. A. Hecker, D. Lundell, J. S. Fine, 3,4-Di-substituted cyclobutene-1,2-diones as CXCR-chemokine receptor ligands. WO2004011418 A, **2004**; e) O. H. Lowry, N. J. Rosebrough, A. L. Farr, R. J. Randall, *J. Biol. Chem.* **1951**, 193, 265–275; f) D. G. Gibson, L. Young, R. Y. Chuang, J. C. Venter, C. A. Hutchison, 3rd, H. O. Smith, *Nat. Methods* **2009**, 6, 343–345; g) M. P. Hall, J. Unch, B. F. Binkowski, M. P. Valley, B. L. Butler, M. G. Wood, P. Otto, K. Zimmerman, G. Vidugiris, T. Machleidt, M. B. Robers, H. A. Benink, C. T. Eggers, M. R. Slater, P. L. Meisenheimer, D. H. Klaubert, F. Fan, L. P. Encell, K. V. Wood, *ACS Chem. Biol.* **2012**, 7, 1848–1857; h) A. Allikalt, N. Purkayastha, K. Flad, M. F. Schmidt, A. Tabor, P. Gmeiner, H. Hübner, D. Weikert, *Sci. Rep.* **2020**, 10, 21842; i) R. Luis, G. D'Uonno, C. B. Palmer, M. Meyrath, T. Uchanski, M. Wantz, B. Rogister, B. Janji, A. Chevigne, M. Szpakowska, *Methods Cell Biol.* **2022**, 169, 279–294; j) M. Meyrath, M. Szpakowska, J. Zeiner, L. Massotte, M. P. Merz, T. Benkel, K. Simon, J. Ohnmacht, J. D. Turner, R. Kruger, V. Seutin, M. Ollert, E. Kostenis, A. Chevigne, *Nat. Commun.* **2020**, 11, 3033; k) A. S. Dixon, M. K. Schwinn, M. P. Hall, K. Zimmerman, P. Otto, T. H. Lubben, B. L. Butler, B. F. Binkowski, T. Machleidt, T. A. Kirkland, M. G. Wood, C. T. Eggers, L. P. Encell, K. V. Wood, *ACS Chem. Biol.* **2016**, 11, 400–408; l) J. C. Shelley, A. Cholleti, L. L. Frye, J. R. Greenwood, M. R. Timlin, M. Uchimaya, *J. Comput.-Aided Mol. Des.* **2007**, 21, 681–691; m) C. Lu, C. Wu, D. Ghoreishi, W. Chen, L. Wang, W. Damm, G. A. Ross, M. K. Dahlgren, E. Russell, C. D. Von Bargen, R. Abel, R. A. Friesner, E. D. Harder, *J. Chem. Theory Comput.* **2021**, 17, 4291–4300; n) G. M. Sastry, M. Adzhigirey, T. Day, R. Annabhimoju, W. Sherman, *J. Comput.-Aided Mol. Des.* **2013**, 27, 221–234; o) R. A. Friesner, J. L. Banks, R. B. Murphy, T. A. Halgren, J. J. Klicic, D. T. Mainz, M. P. Repasky, E. H. Knoll, M. Shelley, J. K. Perry, D. E. Shaw, P. Francis, P. S. Shenkin, *J. Med. Chem.* **2004**, 47, 1739–1749.

Manuscript received: April 19, 2024

Revised manuscript received: June 26, 2024

Accepted manuscript online: June 27, 2024

Version of record online: July 24, 2024